

A Reduction Series of Neodymium Supported by Pyridine Di(imine) Ligands

Shane S. Galley,[§] Scott A. Pattenaude,[§] Robert F. Higgins,[±] Caleb J. Tatebe,[§] Dalton A. Stanley,[§]
Phillip E. Fanwick,[§] Matthias Zeller,[§] Eric J. Schelter,[±] Suzanne C. Bart[§]

[§]H. C. Brown Laboratory of Chemistry, Department of Chemistry, Purdue University, West
Lafayette, Indiana, 47907, United States of America

[±]P. Roy and Diana T. Vagelos Laboratories, Department of Chemistry, University of
Pennsylvania, 231 S. 34th Street, Philadelphia, Pennsylvania 19104, United States.

Contents

Experimental	4
General Considerations	4
Synthesis of ^{Mes}PDI^{Me}NdI₃(THF) (Nd-I₃)	5
Synthesis of ^{Mes}PDI^{Me}NdI₂(THF)₂ (Nd-I₂)	7
Synthesis of ^{Mes}PDI^{Me}NdI(THF)₂ (Nd-I)	9
Synthesis of [^{Mes}PDI^{Me}Nd(THF)]₂ (Nd-THF)	10
Magnetic Data	12
Single Crystal Determinations	17
Figure S1. ¹ H NMR spectrum (CD ₃ CN, ambient temperature) of ^{Mes} PDI ^{Me} NdI ₃ (THF) (Nd-I₃)...6	
Figure S2. Electronic absorption spectrum of Nd-I₃ recorded from 300-800 nm in acetonitrile at ambient temperature.6	
Figure S3. Molecular structure of ^{Mes} PDI ^{Me} NdI ₃ (THF) (Nd-I₃) shown as 30% probability ellipsoids. Hydrogen atoms and co-crystallized solvent molecules omitted for clarity.7	
Figure S4. ¹ H NMR spectrum (C ₆ D ₆ , ambient temperature) of ^{Mes} PDI ^{Me} NdI ₂ (THF) ₂ (Nd-I₂).8	
Figure S5. Electronic absorption spectrum of Nd-I₂ recorded from 300-800 nm in a THF solution at ambient temperature.....8	
Figure S6. ¹ H NMR spectrum (C ₆ D ₆ , ambient temperature) of ^{Mes} PDI ^{Me} NdI(THF) ₂ (Nd-I).9	
Figure S7. Electronic absorption spectrum of Nd-I recorded from 300-800 nm in a THF solution at ambient temperature.10	
Figure S8. ¹ H NMR spectrum (C ₆ D ₆ , ambient temperature) of [^{Mes} PDI ^{Me} Nd(THF)] ₂ (Nd-THF).11	
Figure S9. Electronic absorption spectrum of Nd-THF recorded from 300-800 nm in a THF solution at ambient temperature.....11	
Figure S10. Field dependence of magnetization for Nd-I₃ collected at 100 K.12	
Figure S11. Field dependence of magnetization for Nd-I₂ collected at 100 K.12	
Figure S12. Field dependence of magnetization for Nd-I collected at 100 K.....13	
Figure S13. Field dependence of magnetization for Nd-THF collected at 100 K.13	
Figure S14. Field dependence of magnetization for Nd-I₃ collected at 2 K.13	
Figure S15. Field dependence of magnetization for Nd-I₂ collected at 2 K.14	
Figure S16. Field dependence of magnetization for Nd-I collected at 2 K.....14	
Figure S17. Field dependence of magnetization for Nd-THF collected at 2 K.14	
Figure S18. Temperature dependence of magnetic susceptibility for Nd-I₃ at an applied field of 5000 Oe.....15	
Figure S19. Temperature dependence of magnetic susceptibility for Nd-I₂ at an applied field of 5000 Oe.....15	
Figure S20. Temperature dependence of magnetic susceptibility for Nd-I at an applied field of 5000 Oe.....16	

Figure S21. Temperature dependence of magnetic susceptibility for Nd-THF at an applied field of 1000 Oe.	16
Figure S22. Temperature dependence of the magnetic susceptibility for Nd-I₃ , Nd-I₂ , Nd-I and Nd-THF	17
Figure S23. Molecular structure of Nd-I₃ shown as 30% probability ellipsoids. Hydrogen atoms omitted for clarity.	20
Figure S24. Molecular structure of Nd-I₂ shown as 30% probability ellipsoids. Hydrogen atoms omitted for clarity.	22
Figure S25. Molecular structure of Nd-I shown at 30% probability ellipsoids. Hydrogen atoms omitted for clarity.	24
Figure S26. Molecular structure of Nd-THF shown at 30% probability ellipsoins. Hydrogen atoms omitted for clarity.	26
Table S1. Experimental details for Nd-I₃	19
Table S2. Experimental details for Nd-I₂	21
Table S3. Experimental details for Nd-I	23
Table S4. Experimental details for Nd-THF	25

Experimental

General Considerations

All air- and moisture-sensitive manipulations were performed using standard Schlenk techniques or in an MBraun inert atmosphere drybox with an atmosphere of purified nitrogen. The MBraun drybox was equipped with a cold well designed for freezing samples in liquid nitrogen as well as two -35 °C freezers for cooling samples and crystallizations. Solvents for sensitive manipulations were dried and deoxygenated using literature procedures with a Seca solvent purification system.¹ Benzene-*d*₆ and acetonitrile-*d*₃ were purchased from Cambridge Isotope Laboratories. Deuterated solvents and degassed by three freeze-pump-thaw cycles and stored over molecular sieves. Benzene-*d*₆ was also stored with sodium metal. ^{Mes}PDI^{Me},² KC₈,³ and NdI₃(THF)₃,^{5,4} were prepared according to literature procedures. Neodymium metal was purchased from Strem chemicals.

¹H NMR spectra were recorded on a Varian Inova 300 spectrometer at 299.992 MHz. All chemical shifts are reported relative to the peak for SiMe₄, using ¹H (residual) chemical shifts of the solvent as a secondary standard. The spectra for paramagnetic molecules were obtained by using an acquisition time of 0.5 s; thus the peak widths reported have an error of ±2 Hz. For paramagnetic molecules, the ¹H NMR data are reported with the chemical shift, followed by the peak width at half height in Hertz, the integration value, and, where possible, the peak assignment. Elemental analyses were performed by Complete Analysis Laboratories, Inc., Midwest Microlab, or Robertson Microlit Laboratories.

Magnetic data were collected using a Quantum Design MPMS-7 SQUID (superconducting quantum interface device) magnetometer. Samples were prepared in a dinitrogen filled glovebox (Vacuum Atmospheres, Inc. Nexus II). Powdered samples were loaded into polyethylene bags which were sealed using a Ziploc v159 Vacuum Sealer System. As a precaution, these bags were sealed in another polyethylene bag due to the air and temperature sensitivity of these complexes. The bags were then removed from the glovebox, folded, inserted and immobilized in a plastic drinking straw. The presence (or absence) of ferromagnetic impurities was checked through variable field analyses (0 to 20 kOe) of magnetization at 100 K for each complex (Figures S10-S13). Saturation of magnetization experiments were performed at 2 K varying the applied field from 0 up to

70 kOe (Figures S14-S17). Magnetic susceptibility data were collected at temperatures ranging from 2 to 300 K (Figure S18-S21) at applied fields of 1000 Oe (**Nd-THF**) or 5000 Oe (**Nd-I₃**, **Nd-I₂**, **Nd-I**). Reproducibility of magnetic susceptibility data was checked over two separate batches for each complex measured (Figures S19-S21) except for **Nd-I₃**. Data were corrected for the diamagnetic contributions of the sample holder and bag by subtracting empty containers; corrections for the intrinsic diamagnetism of each sample were calculated from Pascal's constants.⁵

Synthesis of ^{Mes}PDI^{Me}NdI₃(THF) (Nd-I₃**).** A 20 mL scintillation was charged with NdI₃(THF)_{3.5} (0.147 g, 0.189 mmol) and 5 mL toluene. A solution of ^{Mes}PDI^{Me} (0.075 g, 0.189 mmol) in 2 mL toluene was added. This cloudy yellow solution was stirred overnight, causing solubilization of solids. After concentrating the yellow solution *in vacuo*, the resulting yellow residue was washed with pentane (3 x 5 mL) until the pentane washes came out clear. After concentrating *in vacuo*, a yellow powder was obtained and assigned as ^{Mes}PDI^{Me}NdI₃(THF) (**Nd-I₃**) (0.167g, 0.168 mmol, 89%). Crystals were grown from a vapor diffusion of diethyl ether into a concentrated dichloromethane solution at room temperature. Satisfactory elemental analysis results were not possible across multiple attempts.

Elemental Analysis for C₃₁H₃₈N₃OI₃NdO: Calcd C, 37.47; H, 3.85; N, 4.23. Found C, 38.16; H, 3.86; N, 3.75. ¹H NMR (CD₃CN, 25 °C): δ = -5.66 (62, 12H), 1.44 (10, 6H), 1.64 (14, 6H), 1.81 (16, 4H), 3.65 (15, 4H), 4.27 (16, 4H), 15.02 (10, 1H), 16.57 (5, 2H).

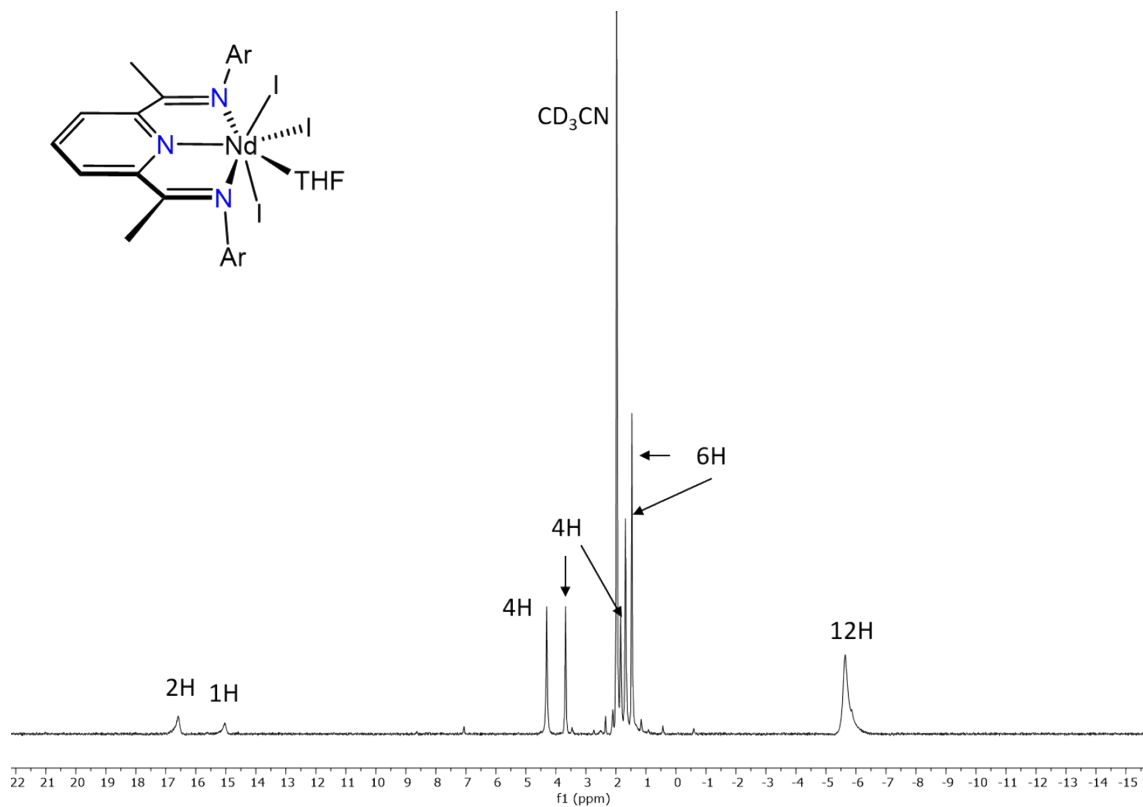


Figure S1. ^1H NMR spectrum (CD_3CN , ambient temperature) of $\text{MesPDI}^{\text{Me}}\text{NdI}_3(\text{THF})$ (**Nd-I₃**).

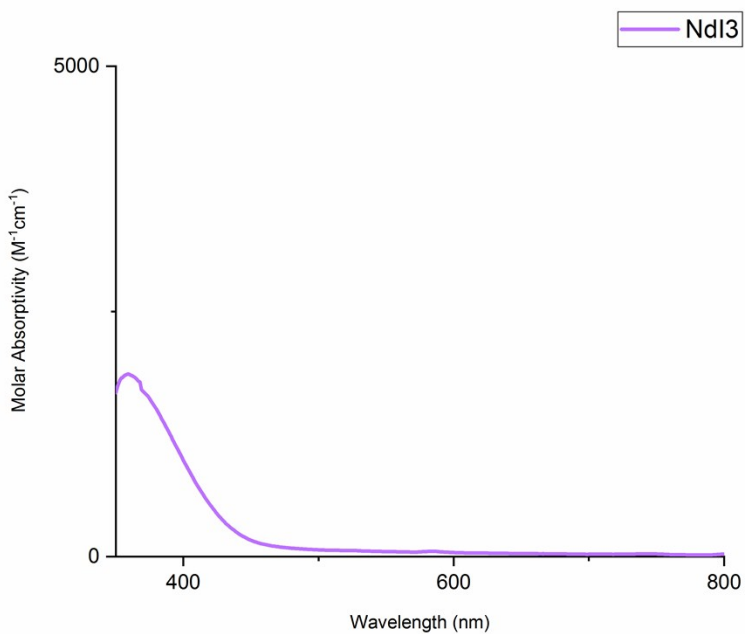


Figure S2. Electronic absorption spectrum of **Nd-I₃** recorded from 300-800 nm in acetonitrile at ambient temperature.

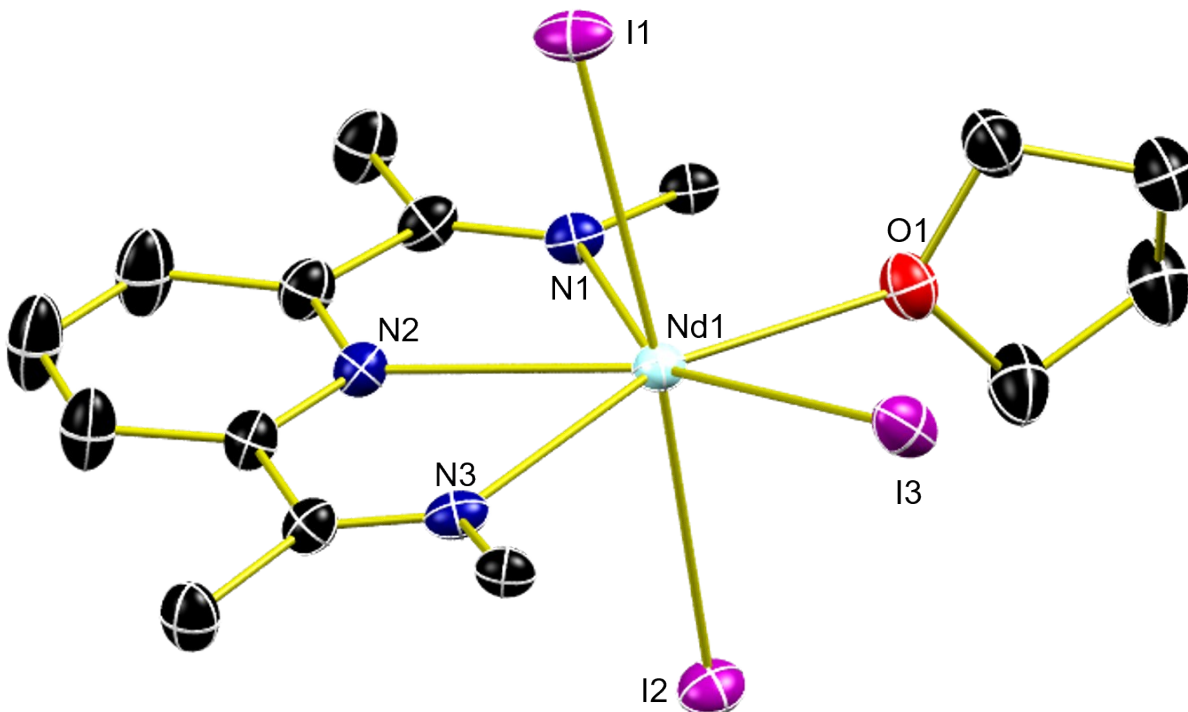


Figure S3. Molecular structure of $\text{MesPDI}^{\text{Me}}\text{NdI}_3(\text{THF})$ (**Nd-I₃**) shown as 30% probability ellipsoids. Hydrogen atoms and co-crystallized solvent molecules omitted for clarity.

Synthesis of $\text{MesPDI}^{\text{Me}}\text{NdI}_2(\text{THF})_2$ (Nd-I₂**).** A 20 mL scintillation vial was charged with $\text{NdI}_3(\text{THF})_{3.5}$ (0.195 g, 0.251 mmol), $\text{MesPDI}^{\text{Me}}$ (0.100 g, 0.251 mmol), and 10 mL of THF. While stirring, KC_8 (0.034, 0.252 mmol) was slowly added, causing an immediate color change to orange. After stirring for one hour, the reaction was filtered over Celite (to remove graphite and KI) and concentrated *in vacuo*, affording a dark residue. To remove any traces residual $\text{MesPDI}^{\text{Me}}$, this residue was washed with *n*-pentane (3 x 10 mL), and dried, giving an orange powder assigned as $\text{MesPDI}^{\text{Me}}\text{NdI}_2(\text{THF})_2$ (**Nd-I₂**) (0.152 g, 0.162 mmol, 83%). Orange crystals suitable for X-ray analysis were grown from a concentrated benzene solution at room temperature.

Elemental Analysis for $\text{C}_{35}\text{H}_{43}\text{N}_3\text{OI}_2\text{Nd}$: Calcd C, 44.83; H, 4.84; N, 4.48. Found C, 44.70; H, 5.00; N, 4.21. ^1H NMR (C_6D_6 , 25 °C): δ = -237.80 (4, 1H, *p*Ar-CH), -8.48 (253, 12H, Mes-CH₃), 2.48 (4, 6H, Mes-CH₃), 5.72 (5, 8H, THF-CH₂), 10.20 (5, 8H, THF-CH₂), 12.72 (9, 4H, Mes-CH), 38.40 (91, 2H, *m*Ar-CH), 189.52 (4, 6H, CH₃).

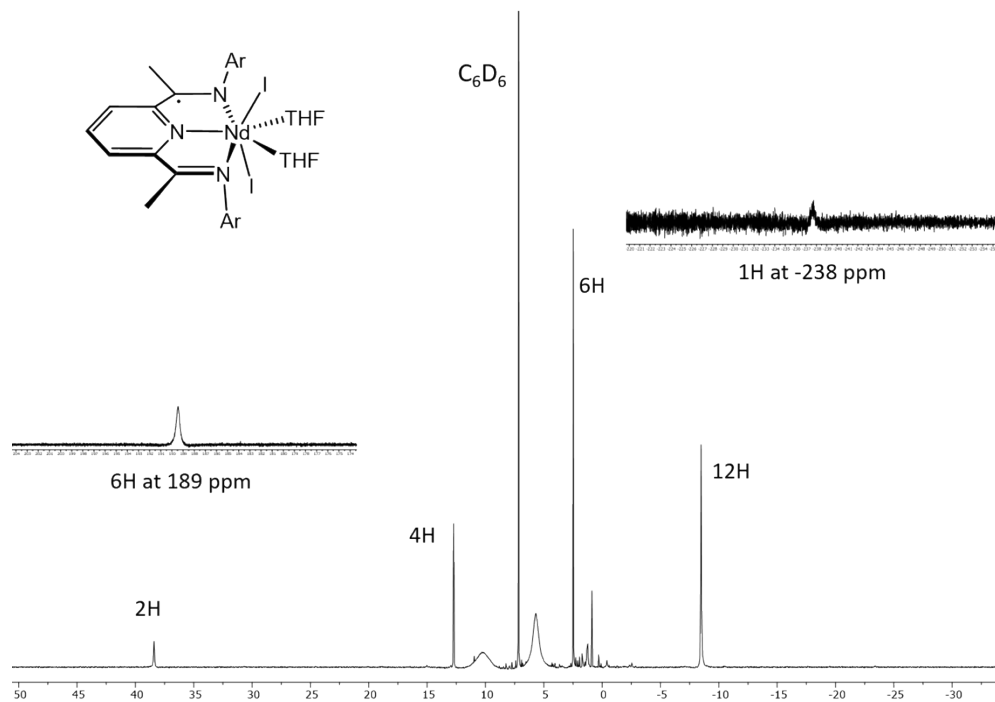


Figure S4. ^1H NMR spectrum (C_6D_6 , ambient temperature) of $\text{MesPDI}^{\text{Me}}\text{NdI}_2(\text{THF})_2$ (**Nd-I₂**).

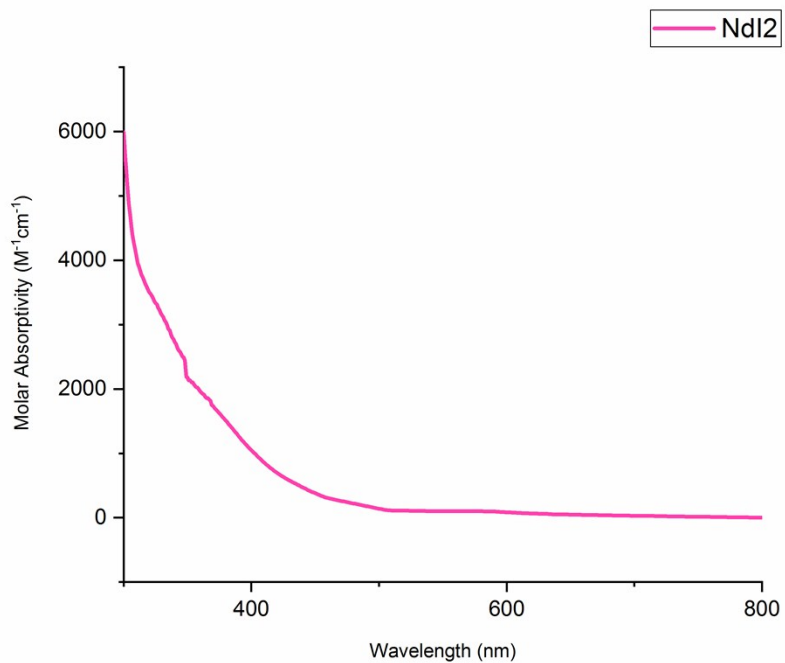


Figure S5. Electronic absorption spectrum of **Nd-I₂** recorded from 300-800 nm in a THF solution at ambient temperature.

Synthesis of $^{\text{Mes}}\text{PDI}^{\text{Me}}\text{NdI}(\text{THF})_2$ (Nd-I**).** A 20 mL scintillation was charged with $\text{NdI}_3(\text{THF})_{3.5}$ (0.250 g, 0.322 mmol), $^{\text{Mes}}\text{PDI}^{\text{Me}}$ (0.128 g, 0.322 mmol), and 15 mL of THF, creating a slurry. While stirring, KC_8 (0.087, 0.644 mmol) was slowly added as a solid, causing an immediate color change to dark-orange. After stirring for one hour, the reaction was filtered (to remove graphite and KI) and concentrated in vacuo to a dark residue. To remove any traces of free $^{\text{Mes}}\text{PDI}^{\text{Me}}$, this residue was washed with pentane (3 x 12 mL), and again concentrated in vacuo to a dark-orange powder assigned as $^{\text{Mes}}\text{PDI}^{\text{Me}}\text{NdI}(\text{THF})_2$ (**Nd-I**) (0.144 g, 0.177 mmol, 55%). Orange single crystals suitable for X-ray analysis were grown from a concentrated Et_2O solution cooled to -35 °C. Satisfactory elemental analysis results were not possible, as a result of incomplete combustion.

Elemental Analysis for $\text{C}_{35}\text{H}_{47}\text{N}_3\text{O}_2\text{INd}$: Calcd C, 51.71; H, 5.83; N, 5.17. Found C, 50.03; H, 5.83; N, 4.87. ^1H NMR (C_6D_6 , 25 °C): $\delta = -43$ (7), -14.59 (3), -13.70 (5), -8.23 (3), -1.62 (5), 5.55 (5), 12.92 (3), 19.86 (3), 21.96 (5), 28.26 (3), 39.08 (2), 188.90 (3).

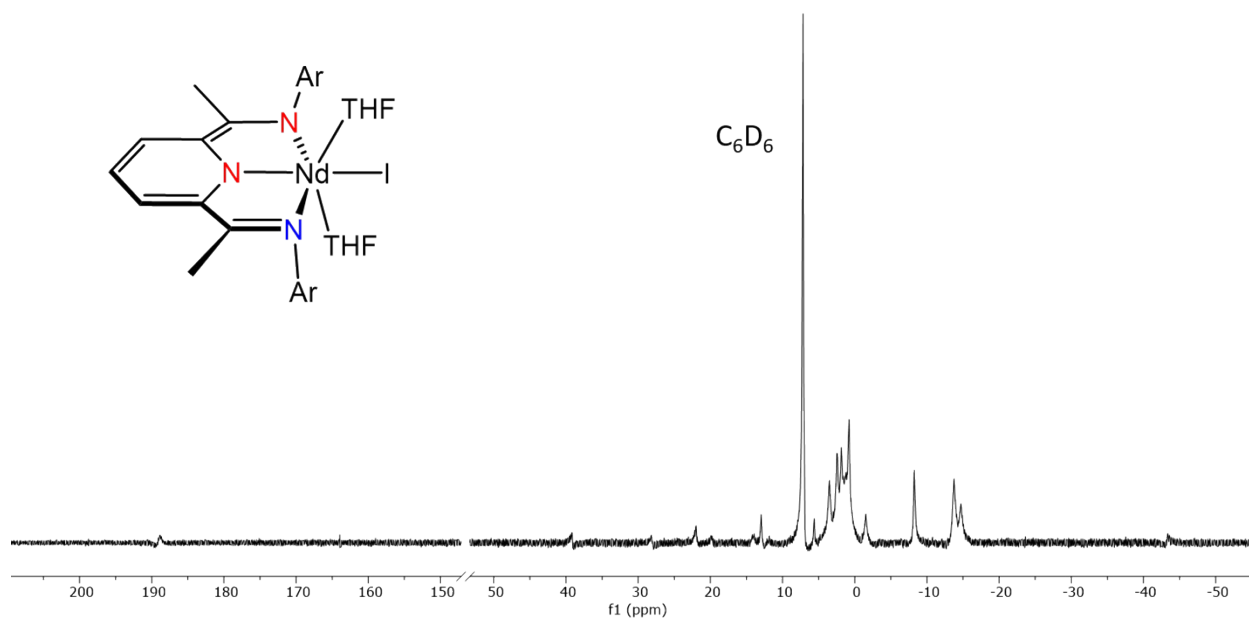


Figure S6. ^1H NMR spectrum (C_6D_6 , ambient temperature) of $^{\text{Mes}}\text{PDI}^{\text{Me}}\text{NdI}(\text{THF})_2$ (**Nd-I**).

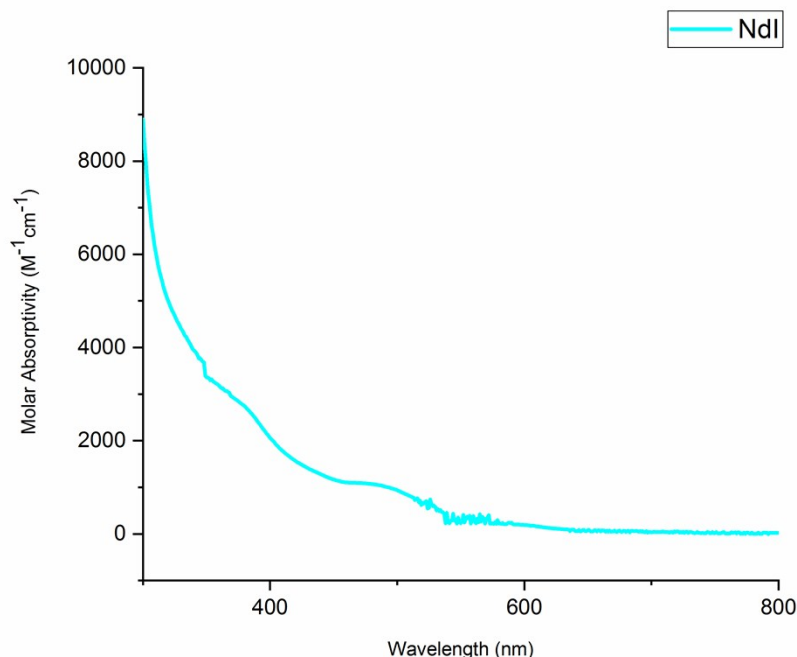


Figure S7. Electronic absorption spectrum of **Nd-I** recorded from 300-800 nm in a THF solution at ambient temperature.

Synthesis of $[\text{MesPDI}^{\text{Me}}\text{Nd}(\text{THF})]_2$ (Nd-THF**).** A 20 mL scintillation was charged with $\text{NdI}_3(\text{THF})_{3.5}$ (0.150 g, 0.251 mmol), $\text{MesPDI}^{\text{Me}}$ (0.076 g, 0.251 mmol), and 12 mL of THF, creating a slurry. While stirring, KC_8 (0.078, 0.252 mmol) was slowly added as a solid, causing an immediate color change to dark brown-green. After stirring for one hour, the reaction was filtered over Celite (to remove graphite and KI) and concentrated *in vacuo* to a dark residue. To remove any traces of bis($\text{MesPDI}^{\text{Me}}$) product, this residue was washed with pentane (6 x 10 mL), and again concentrated *in vacuo* to an emerald green powder assigned as $[\text{MesPDI}^{\text{Me}}\text{Nd}(\text{THF})]_2$ (**Nd-THF**) (0.100 g, 0.081 mmol, 65%). Green single crystals suitable for X-ray analysis were grown from a concentrated Et_2O solution cooled to $-35\text{ }^\circ\text{C}$. Satisfactory elemental analysis results were not possible, as a result of incomplete combustion.

Elemental Analysis for $\text{C}_{62}\text{H}_{78}\text{N}_6\text{O}_2\text{Nd}_2$: Calcd C, 60.65; H, 6.40; N, 6.84. Found C, 58.07; H, 6.49; N, 6.68. ^1H NMR (C_6D_6 , $25\text{ }^\circ\text{C}$): $\delta = -479.37$ (5, 1H, *pAr-CH*), -6.16 (103, 6H, *Mes-CH*₃), 2.56 (14, 8H, *THF-CH*₂), 3.22 (26, 8H, *THF-CH*₂), 7.34 (8, 6H, *Mes-CH*₃), 10.73 (15, 6H, *Mes-CH*₃), 14.22 (9, 2H, *Mes-CH*), 30.28 (110, 2H, *Mes-CH*), 160.74 (5, 2H, *mAr-CH*), 227.31 (5, 6H, *CH*₃).

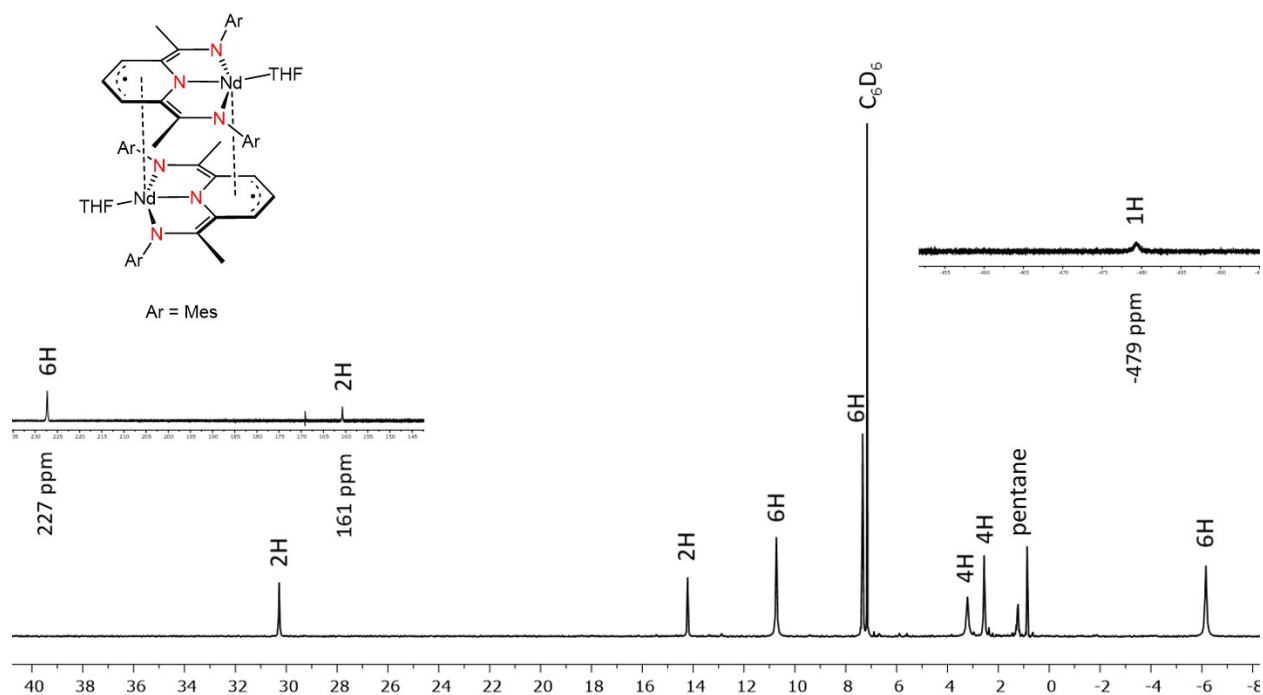


Figure S8. ^1H NMR spectrum (C_6D_6 , ambient temperature) of $[\text{MesPDI}^{\text{Me}}\text{Nd}(\text{THF})_2]$ (**Nd-THF**).

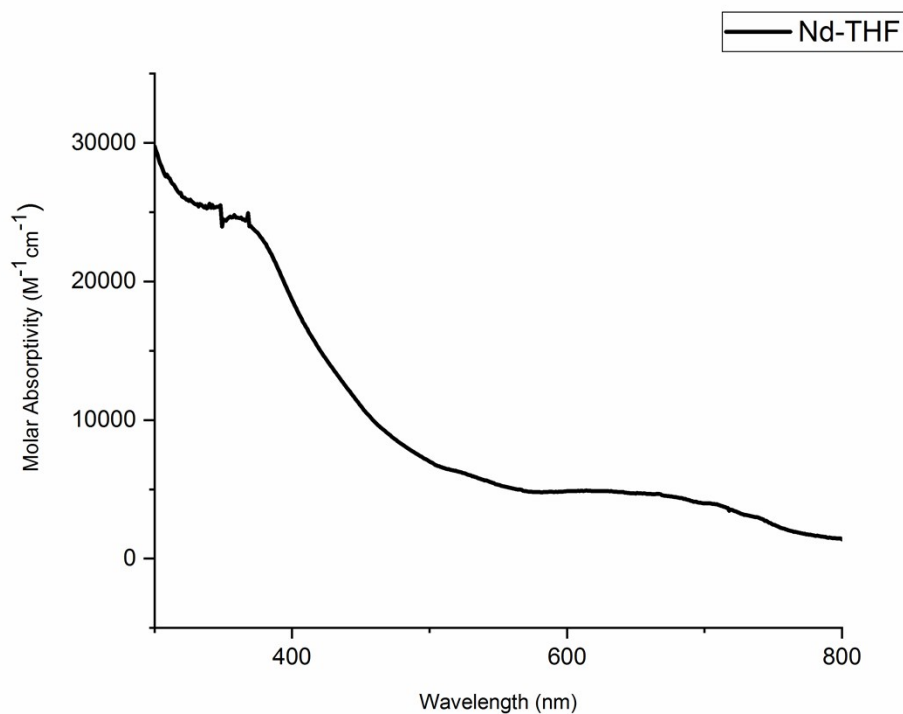


Figure S9. Electronic absorption spectrum of **Nd-THF** recorded from 300-800 nm in a THF solution at ambient temperature.

Magnetic Data

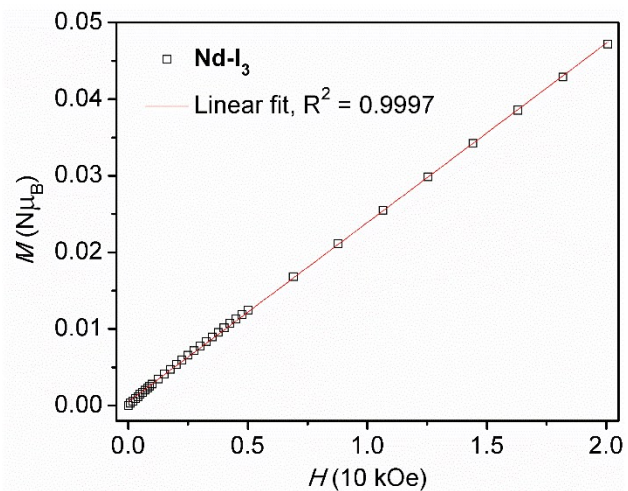


Figure S10. Field dependence of magnetization for **Nd-I₃** collected at 100 K.

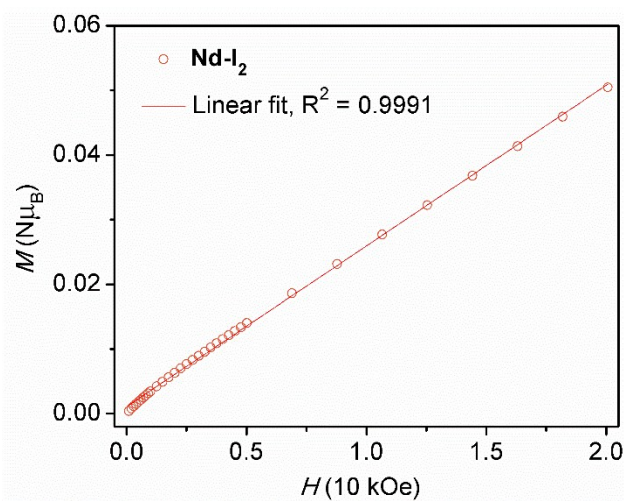


Figure S11. Field dependence of magnetization for **Nd-I₂** collected at 100 K.

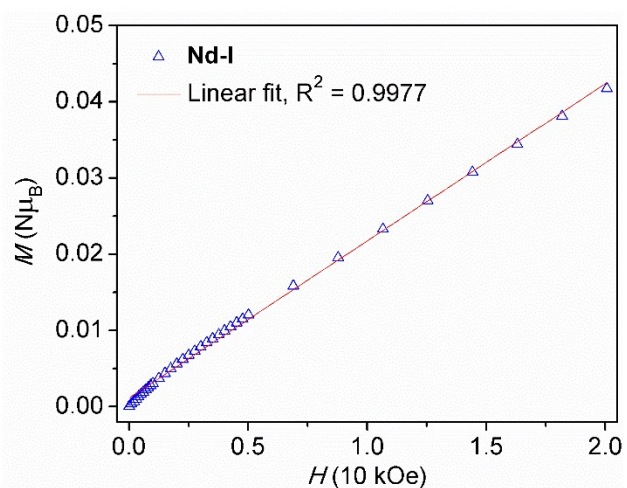


Figure S12. Field dependence of magnetization for **Nd-I** collected at 100 K.

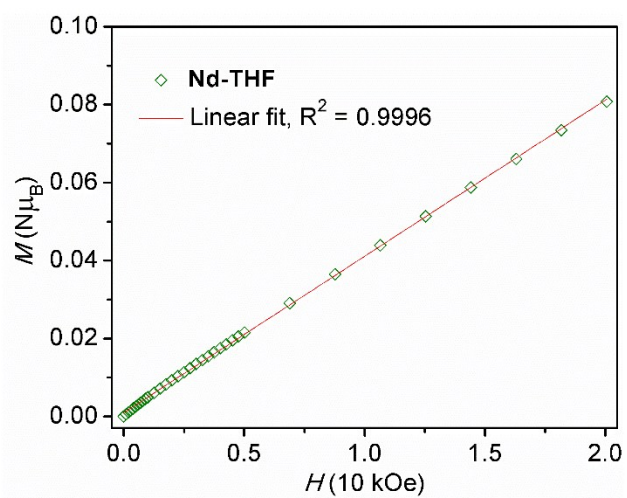


Figure S13. Field dependence of magnetization for **Nd-THF** collected at 100 K.

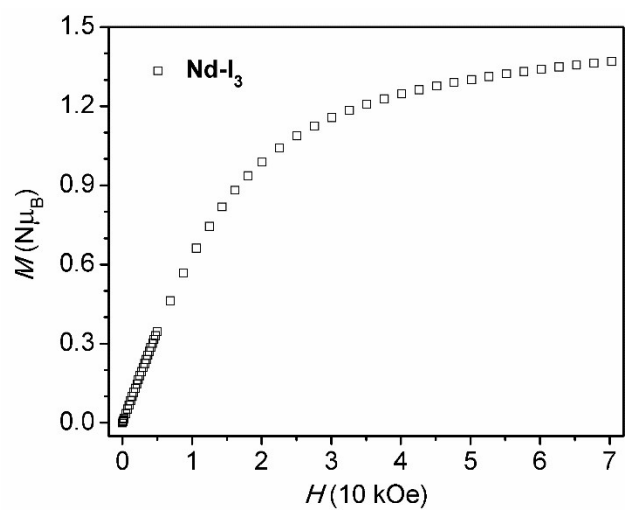


Figure S14. Field dependence of magnetization for **Nd-I₃** collected at 2 K.

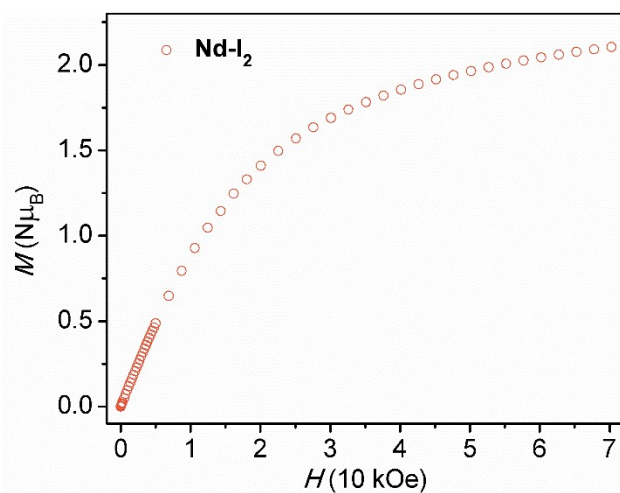


Figure S15. Field dependence of magnetization for **Nd-I₂** collected at 2 K.

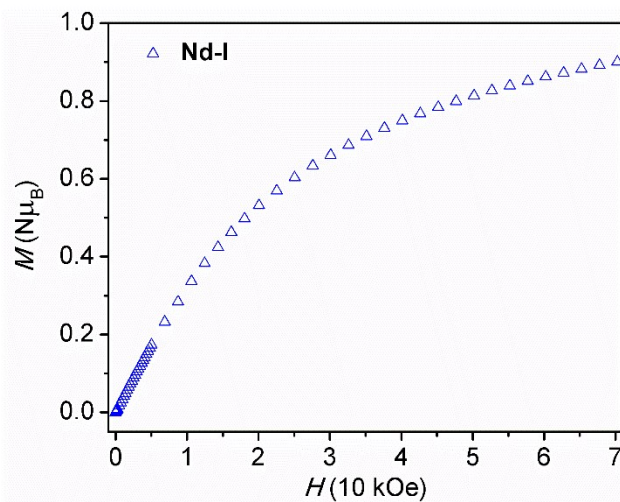


Figure S16. Field dependence of magnetization for **Nd-I** collected at 2 K.

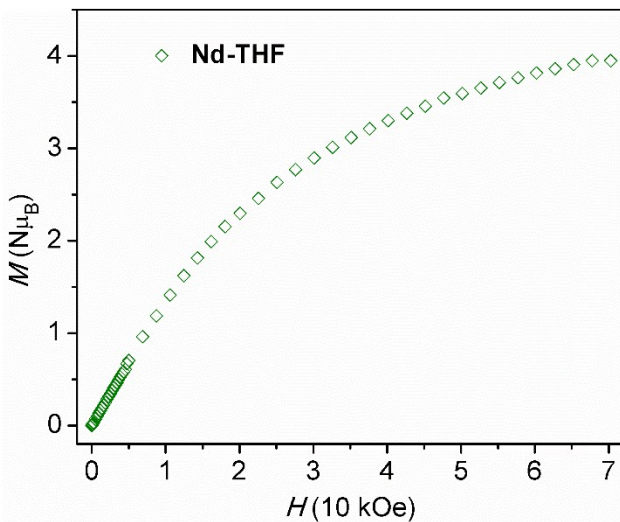


Figure S17. Field dependence of magnetization for **Nd-THF** collected at 2 K.

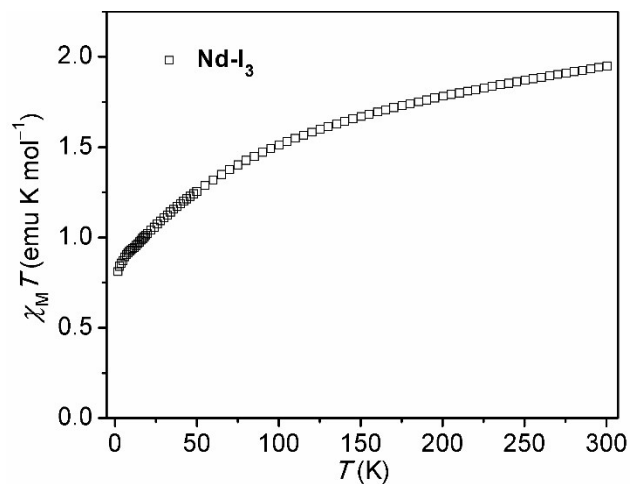


Figure S18. Temperature dependence of magnetic susceptibility for **Nd-I₃** at an applied field of 5000 Oe.

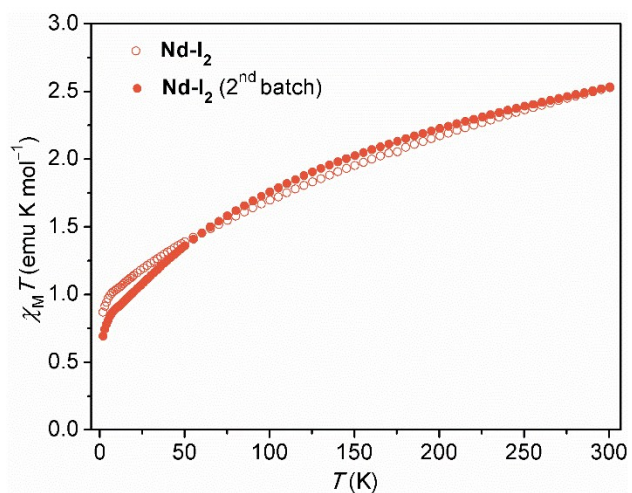


Figure S19. Temperature dependence of magnetic susceptibility for **Nd-I₂** at an applied field of 5000 Oe.

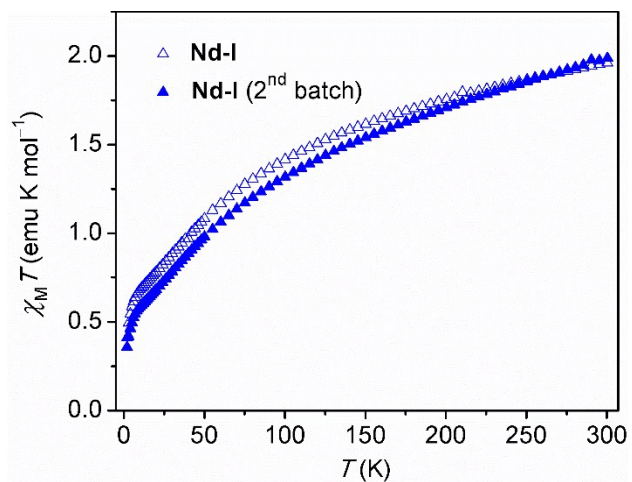


Figure S20. Temperature dependence of magnetic susceptibility for **Nd-I** at an applied field of 5000 Oe.

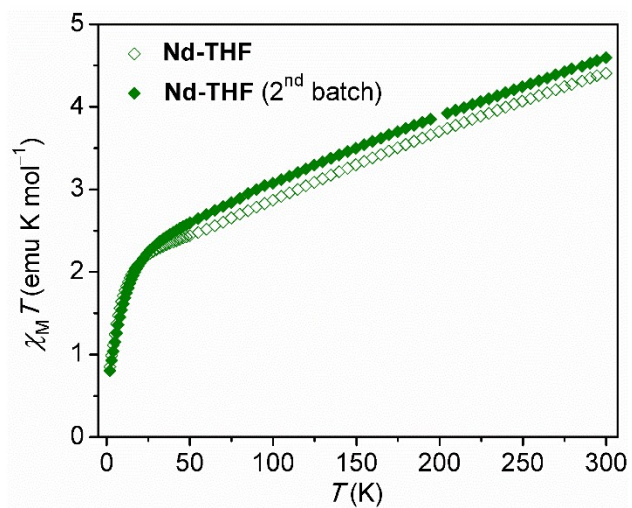


Figure S21. Temperature dependence of magnetic susceptibility for **Nd-THF** at an applied field of 1000 Oe.

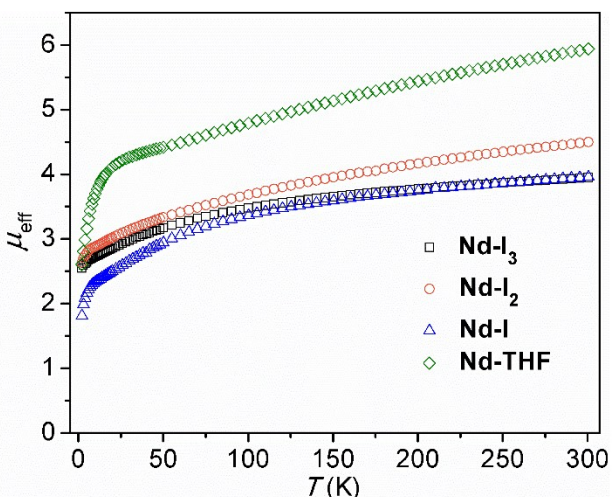


Figure S22. Temperature dependence of the magnetic susceptibility for **Nd-I₃**, **Nd-I₂**, **Nd-I** and **Nd-THF**.

Single Crystal Determinations

Single crystals of **Nd-I** and **Nd-THF** suitable for X-ray diffraction were coated with poly(isobutylene) oil in a glovebox and quickly transferred to the goniometer head of a Rigaku Rapid II image plate diffractometer equipped with a MicroMax002+ high intensity copper X-ray source with confocal optics. Preliminary examination and data collection were performed with Cu K α radiation ($\lambda = 1.54184 \text{ \AA}$) with the omega scan technique. In a similar manner, single crystals of **Nd-I₃** and **Nd-I₂** were transferred to the goniometer head of a Nonius Kappa CCD diffractometer equipped with a graphite crystal and incident beam monochromator and examined with Mo K α radiation ($\lambda = 0.71073 \text{ \AA}$).

Data were collected using the Nonius Collect⁶ or CrystalClear software.⁷ These data sets were processed using HKL3000⁸ and data were corrected for absorption and scaled using Scalepack.⁸ The space groups were assigned and the structures were solved by direct methods using XPREP within the SHELXTL suite of programs⁹ and refined by full matrix least squares against F^2 with all reflections with Shelxl2016¹⁰ using the graphical interface Shelxle.¹¹ If not specified otherwise, H atoms attached to carbon atoms were positioned geometrically and constrained to ride on their parent atoms, with carbon hydrogen bond distances of 0.95 \AA for aromatic C-H and 1.00, 0.99 and 0.98 \AA for aliphatic C-H, CH₂, and CH₃ moieties, respectively. Methyl H atoms were allowed to rotate but not to tip to best fit the experimental electron density.

$U_{\text{iso}}(\text{H})$ values were set to a multiple of $U_{\text{eq}}(\text{C})$ with 1.5 for CH_3 , and 1.2 for CH_2 , and C-H units, respectively. Additional data collection and refinement details, including description of disorder (where present) can be found with the individual structure descriptions, below. Complete crystallographic data, in CIF format, have been deposited with the Cambridge Crystallographic Data Centre. CCDC 1897067-1897069, 1906417 contains the supplementary crystallographic data for this paper. These data can be obtained free of charge from The Cambridge Crystallographic Data Centre via www.ccdc.cam.ac.uk/data_request/cif.

CCDC: 1906417

Local name: ssg0324NdI3thf_0m

Table S1. Experimental details for **Nd-I₃**.

Crystal data	
Chemical formula	C ₃₁ H ₃₉ I ₃ N ₃ NdO
M_r	994.59
Crystal system, space group	Monoclinic, $P2_1/n$
Temperature (K)	150
a, b, c (Å)	10.8314 (7), 16.2124 (8), 20.5519 (13)
β (°)	103.4083 (18)
V (Å ³)	3510.6 (4)
Z	4
Radiation type	Mo $K\alpha$
μ (mm ⁻¹)	4.14
Crystal size (mm)	0.83 × 0.59 × 0.42
Data collection	
Diffractometer	Bruker AXS D8 Quest CMOS diffractometer
Absorption correction	Multi-scan <i>SADABS</i> 2016/2 ¹²
T_{\min}, T_{\max}	0.058, 0.100
No. of measured, independent and observed [$I > 2\sigma(I)$] reflections	91004, 11017, 8292
R_{int}	0.049
$(\sin \theta/\lambda)_{\text{max}}$ (Å ⁻¹)	0.722
Refinement	
$R[F^2 > 2\sigma(F^2)], wR(F^2), S$	0.037, 0.094, 1.05
No. of reflections	11017
No. of parameters	479
No. of restraints	523
H-atom treatment	H-atom parameters constrained
	$w = 1/[\sigma^2(F_o^2) + (0.0326P)^2 + 10.2951P]$ where $P = (F_o^2 + 2F_c^2)/3$
$\Delta\rho_{\text{max}}, \Delta\rho_{\text{min}}$ (e Å ⁻³)	1.10, -0.98

Computer programs: Apex3 v2016.9-0,¹³ *SAINT* V8.37A,¹⁴ *SHELXS97*,⁹ *SHELXL2018/3*.¹¹

Refinement details:

Disorder was introduced by the ligand causing shift in the metal, THF, and iodines. The ligand backbone, iodines, THF, and metal center was modeled to have partial disorder. SADI command was used to keep the ligand and metal bond distance the same. The FLAT command was used to keep the ligand backbone in plane.

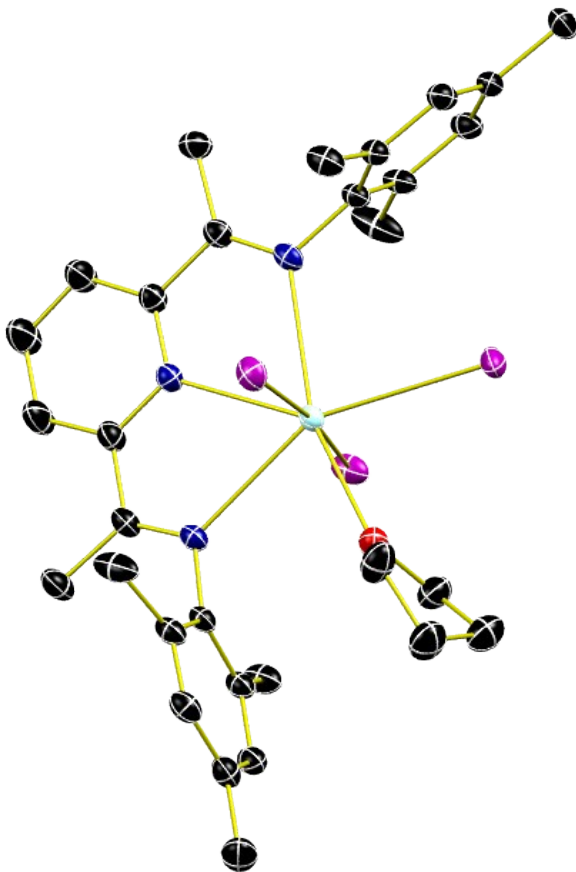


Figure S23. Molecular structure of Nd-I₃ shown as 30% probability ellipsoids. Hydrogen atoms omitted for clarity.

CCDC: 1897067

Local name: SAP208_2019

Table S2. Experimental details for **Nd-I₂**.

Crystal data	
Chemical formula	C ₃₅ H ₄₇ I ₂ N ₃ NdO ₂ ·2(C ₆ H ₆)
<i>M_r</i>	1096.01
Crystal system, space group	Monoclinic, <i>P</i> 2 ₁
Temperature (K)	150
<i>a</i> , <i>b</i> , <i>c</i> (Å)	11.0654 (9), 15.4966 (7), 14.2383 (15)
β (°)	110.339 (4)
<i>V</i> (Å ³)	2289.3 (3)
<i>Z</i>	2
Radiation type	Mo Kα
μ (mm ⁻¹)	2.52
Crystal size (mm)	0.42 × 0.30 × 0.24
Data collection	
Diffractometer	Nonius KappaCCD
Absorption correction	Multi-scan <i>SCALEPACK</i> ⁸
<i>T_{min}</i> , <i>T_{max}</i>	0.078, 0.546
No. of measured, independent and observed [<i>I</i> > 2σ(<i>I</i>)] reflections	10043, 10043, 8589
<i>R_{int}</i>	0.036
(sin θ/λ) _{max} (Å ⁻¹)	0.665
Refinement	
<i>R</i> [<i>F</i> ² > 2σ(<i>F</i> ²)], <i>wR</i> (<i>F</i> ²), <i>S</i>	0.036, 0.079, 1.06
No. of reflections	10043
No. of parameters	480
No. of restraints	1
H-atom treatment	H-atom parameters constrained
Δρ _{max} , Δρ _{min} (e Å ⁻³)	1.06, -1.26
	$w = 1/[\sigma^2(\text{Fo}^2) + (0.0237\text{P})^2 + 2.6948\text{P}]$ where $\text{P} = (\text{Fo}^2 + 2\text{Fc}^2)/3$
Absolute structure	Flack ¹⁵ x determined using 3235 quotients [(<i>I</i> +)-(<i>I</i> -)]/[(<i>I</i> +)+(<i>I</i> -)]

Absolute structure parameter	0.017 (10)
------------------------------	------------

Computer programs: Nonius Collect,⁶ *HKL-3000*,⁸ *SHELXT*,⁹ *SHELXL2018/3*.¹⁰

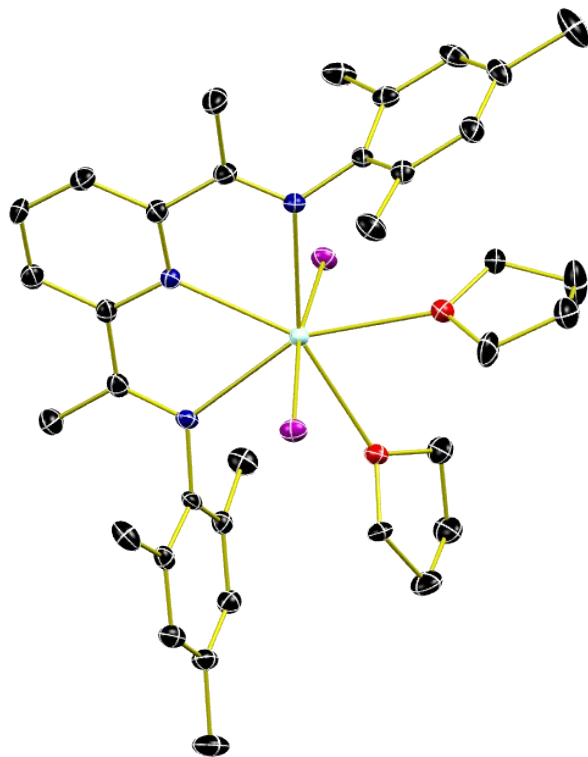


Figure S24. Molecular structure of **Nd-I₂** shown as 30% probability ellipsoids. Hydrogen atoms omitted for clarity.

CCDC: 1897069

Local name: sap383_sq

Table S3. Experimental details for Nd-I.

Crystal data	
Chemical formula	C ₃₅ H ₄₇ IN ₃ NdO ₂
M_r	812.89
Crystal system, space group	Monoclinic, $P2_1/n$
Temperature (K)	100
a, b, c (Å)	8.8201 (8), 22.84050 (17), 18.48220 (11)
β (°)	96.758 (6)
V (Å ³)	3697.5 (3)
Z	4
Radiation type	Cu $K\alpha$
μ (mm ⁻¹)	17.50
Crystal size (mm)	0.25 × 0.15 × 0.10
Data collection	
Diffractometer	Rigaku Rapid II curved image plate diffractometer
Absorption correction	Multi-scan <i>SCALEPACK</i> ⁸
T_{\min}, T_{\max}	0.052, 0.273
No. of measured, independent and observed [$I > 2\sigma(I)$] reflections	46988, 6632, 4597
R_{int}	0.159
$(\sin \theta/\lambda)_{\text{max}}$ (Å ⁻¹)	0.610
Refinement	
$R[F^2 > 2\sigma(F^2)], wR(F^2), S$	0.100, 0.297, 1.07
No. of reflections	6632
No. of parameters	480
No. of restraints	378
H-atom treatment	H-atom parameters constrained
	$w = 1/[\sigma^2(F_o^2) + (0.1406P)^2 + 40.3641P]$ where $P = (F_o^2 + 2F_c^2)/3$
$\Delta\rho_{\text{max}}, \Delta\rho_{\text{min}}$ (e Å ⁻³)	1.83, -1.75

Computer programs: *CrystalClear-SM* Expert 2.1 b32,⁷ *HKL-3000*,⁸ *SHELXS97*,⁹

SHELXL2014/7,¹⁰ *SHELXLE Rev794*.¹¹

Refinement notes: Two THF molecules and the iodine atom were refined as disordered, with the iodine atom and one of the THF molecules sharing a common occupancy ratio. The four THF moieties were restrained to have similar geometries, and U^{ij} components of ADPs were restrained to be similar for atoms closer than 2.0 Å. One of the oxygen atoms was omitted from the disorder. The occupancy ratios refined to 0.67(2) to 0.33(2) for the first THF, and to 0.693(15) to 0.307(15) for the second THF and the iodine.

The structure contains two independent solvent accessible voids of 144 Å³ each. No substantial electron density peaks were found in the solvent accessible voids (less than two electrons per cubic Å) and the residual electron density peaks are not arranged in an interpretable pattern. The hkl file was instead corrected using reverse Fourier transform methods using the SQUEEZE routine^{16, 17} as implemented in Platon. The resultant files were used in the further refinement. (The FAB file with details of the Squeeze results is appended to this cif file). The Squeeze procedure corrected for 60 electrons within the solvent accessible voids.

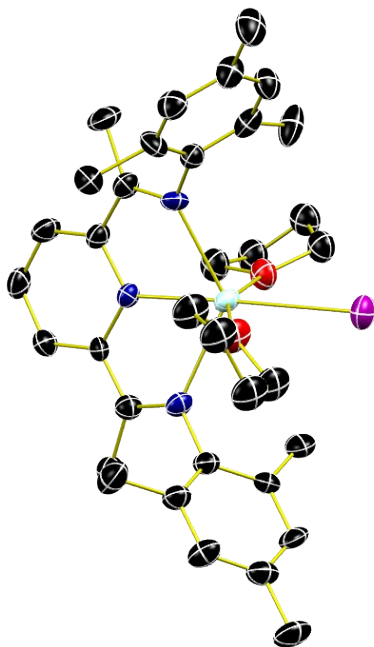


Figure S25. Molecular structure of **Nd-I** shown at 30% probability ellipsoids. Hydrogen atoms omitted for clarity.

CCDC: 1897068

Local name: sap387

Table S4. Experimental details for **Nd-THF**.

Crystal data	
Chemical formula	$C_{62}H_{78}N_6Nd_2O_2 \cdot C_4H_{10}O$
M_r	1301.90
Crystal system, space group	Monoclinic, $P2_1/c$
Temperature (K)	100
a, b, c (Å)	11.2456 (5), 15.8225 (9), 16.9949 (7)
β (°)	93.319 (3)
V (Å ³)	3018.9 (3)
Z	2
Radiation type	Cu $K\alpha$
μ (mm ⁻¹)	13.35
Crystal size (mm)	0.09 × 0.08 × 0.06
Data collection	
Diffractometer	Rigaku Rapid II curved image plate diffractometer
Absorption correction	Multi-scan <i>SCALEPACK</i> ⁸
T_{min}, T_{max}	0.369, 0.501
No. of measured, independent and observed [$I > 2\sigma(I)$] reflections	31954, 5576, 4106
R_{int}	0.101
$(\sin \theta/\lambda)_{max}$ (Å ⁻¹)	0.618
Refinement	
$R[F^2 > 2\sigma(F^2)], wR(F^2), S$	0.057, 0.142, 1.10
No. of reflections	5576
No. of parameters	381
No. of restraints	27
H-atom treatment	H-atom parameters constrained
	$w = 1/[\sigma^2(F_o^2) + (0.0451P)^2 + 13.2199P]$ where $P = (F_o^2 + 2F_c^2)/3$
$\Delta\rho_{max}, \Delta\rho_{min}$ (e Å ⁻³)	1.21, -1.41

Computer programs: *CrystalClear-SM* Expert 2.1 b32 (Rigaku, 2014), *HKL-3000*

(Otwinowski & Minor, 1997), *SHELXS97* (Sheldrick, 2008), *SHELXL2014/7* (Sheldrick, 2014), *SHELXLE Rev761* (Hübschle *et al.*, 2011).

Refinement notes: A diethyl ether molecule is disordered across an inversion center. Equivalent bond distances and 1,3 distances were restrained to be similar, and U^{ij} components of ADPs of disordered atoms were restrained to be similar.

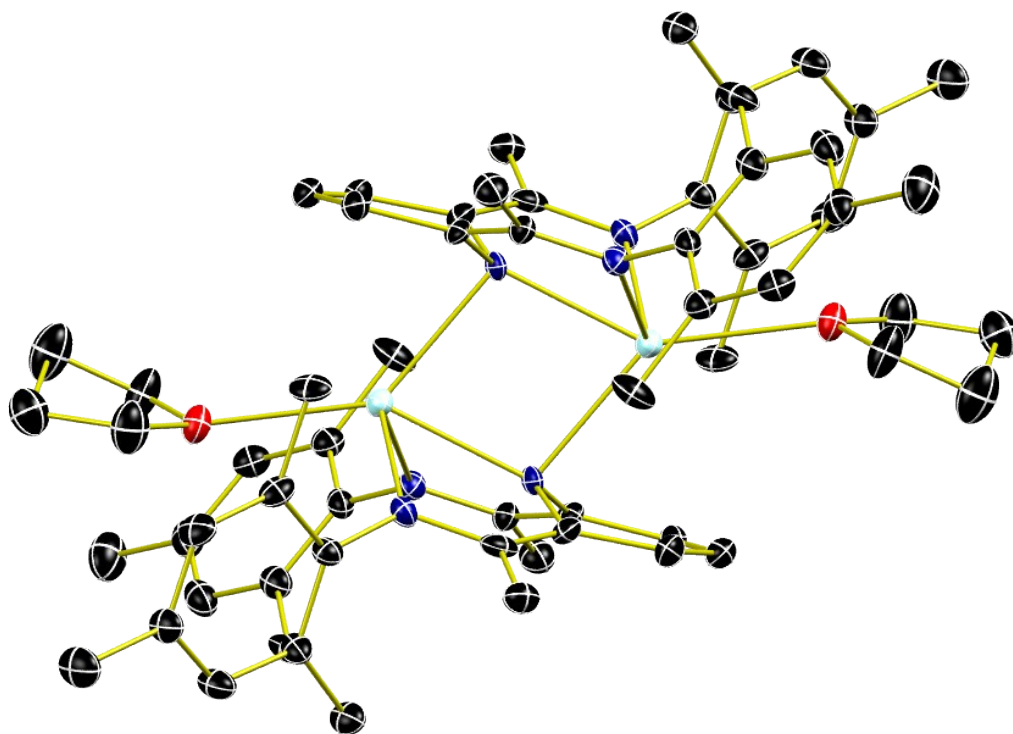


Figure S26. Molecular structure of **Nd-THF** shown at 30% probability ellipsoids. Hydrogen atoms omitted for clarity.

References

1. A. B. Pangborn, M. A. Giardello, R. H. Grubbs, R. K. Rosen and F. J. Timmers, *Organometallics*, 1996, **15**, 1518-1520.
2. G. J. P. Britovsek, M. Bruce, V. C. Gibson, B. S. Kimberley, P. J. Maddox, S. Mastroianni, S. J. McTavish, C. Redshaw, G. A. Solan, S. Strömberg, A. J. P. White and D. J. Williams, *Journal of the American Chemical Society*, 1999, **121**, 8728-8740.
3. C. Soma, C. Jayanta, G. Wenhua and B. W. Edward, *Angewandte Chemie International Edition*, 2007, **46**, 4486-4488.
4. K. Izod, S. T. Liddle and W. Clegg, *Inorganic Chemistry*, 2004, **43**, 214-218.
5. G. A. Bain and J. F. Berry, *Journal of Chemical Education*, 2008, **85**, 532.
6. *Journal*, 1998.
7. *Journal*, 1998.
8. Z. Otwinowski and W. Minor, *Methods in Enzymology*, 1997, **276**, 307-326.
9. G. M. Sheldrick, *Acta Crystallogr A*, 2008, **64**, 112-122.
10. G. M. Sheldrick, *Acta Crystallogr C Struct Chem*, 2015, **71**, 3-8.
11. C. B. Hubschle, G. M. Sheldrick and B. Dittrich, *J Appl Crystallogr*, 2011, **44**, 1281-1284.
12. L. Krause, R. Herbst-Irmer, G. M. Sheldrick and D. Stalke, *Journal of Applied Crystallography*, 2015, **48**, 3-10.
13. *Journal*, 2016.
14. *Journal*, 2015.
15. S. Parsons, H. D. Flack and T. Wagner, *Acta Crystallographica Section B*, 2013, **69**, 249-259.
16. A. L. Spek, *Acta Crystallogr C Struct Chem*, 2015, **71**, 9-18.
17. P. van der Sluis and A. L. Spek, *Acta Crystallographica Section A*, 1990, **46**, 194-201.